DESIGN OF SWITCHED RELUCTANCE MOTOR USING RELUCTANCE NETWORK ANALYSIS COMBINED TO TEETH CONTOUR PERMEANCE METHOD.

N.KADA BELGHITRI A.TAIEB BRAHIMI
C.KERNANE
Department of Electrical Engineering
Faculty of Electrical Engineering
University of Science and Technology Mohamed Boudiaf
B. P 1505 - Oran El - Mnaouer 31000 – Algéria.
kabelnaw@yahoo.fr, ataieb_brahim@yahoo.fr, chafikkernane@hotmail.com.

Abstract: *In this paper a design procedure for 6/4 switched reluctance motor is established. A 2D non-linear reluctance network model combined to teeth contour permeance method is used. A calculation algorithm was first implemented on the basis of existing motor and then extended for varying dimensions of geometric parameters, specially teeth and air gap. The model was validated with finite elements analysis. The design procedure was established on the basis of minimizing torque ripples. The study contains two parts; a constant current supplied motor then a constant voltage supplied one. Finally a relation between stator teeth and rotor teeth with the airgap as parameter was established.*

Keywords: *Coenergie, non-linear model, Reluctance network method, Switched reluctance motor, teeth contour permeance.*

1. Introduction.

Switched reluctance motors (SRM) are used in many applications (electric vehicles, wind energy, aeronautics…etc.) due to their simple construction, robustness, low cost and ability to operate over a wide speed range and a wide motor power ratings , using both two quadrant and four quadrant operation.The development of power electronics also allowed growing interest for this kind of motors. Many papers treated the SRM design using classical methods like finite element method or analytical methods for modelisation.

Reluctance network method (RNM) is also widely used but the calculation of airgap reluctance still complicated since it is position dependent.

In this paper (RNM) is combined to teeth contour permeances method to calculate this airgap reluctance. The reluctance network method (RNM) consists of dividing the machine into parts represented by reluctances where field is assumed to be normal to the cross section. These parts are yokes, teeth, slots, and airgap. This method allows improving calculation speed, keeping accuracy and flexibility.The aim is to highlight the effects of changing stator and rotor teeth dimensions on torque characteristics. An algorithm taking into account all configurations of airgap and position is implemented, and it is for all dimensions and positions of rotor for a 6/4 SRM [1-2].

The SRM studied contains 6 stator poles with concentric windings. Two diametrically opposite poles windings are in series to form a phase. The rotor has 4 salient poles but no active element (Figure 1). Two important positions are to be considered in this type of motors; the position (0°) of non-alignment of the axis of both stator and rotor tooth and the position of alignment (30°) of these two axes (figure 1). Supplying with constant voltage or constant current phase (A)(in red) when rotor pole 1 is at position (0°) ,generates a main magnetic flux that gives rise to an electromagnetic reluctant torque. The rotor pole 1 is pulled in order to reduce the airgap reluctance. Supplying three successive phases causes a continuous movement of the rotor.

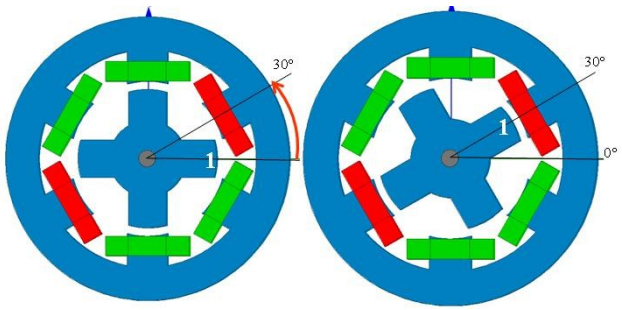

Fig. 1. Geometric configuration and operation of SRM.

SRM needs a supply device that must take into consideration three important positions; θ_{on} the supply angle, θ_{off} the turning off angle and θ_{ext} the angle when the current in the windings becomes to zero. These characteristic angles need a performing electric drive, but in this work and for convenience the drive simply delivers a step current or voltage between θ_{on} and θ_{off} and inversed between θ_{off} *and* θ_{ext} .The voltage supply function is given by equation (1):

$$U_1(\theta) = \begin{cases} 80V & \theta_{on} \le \theta \le \theta_{offt} \\ -80V & \theta_{off} \le \theta \le \theta_{ext} \end{cases} \quad (1)$$

The motor electromagnetic parameters are highly non-linear due to nonlinearity of magnetic material and the air gap configuration which is strongly salient. To reduce complexity and simplify the modelisation, the ends effect, magnetic losses and hysteresis losses are neglected. The electromagnetic differential equation for the motor is given by [3,4,6]:

$$\begin{aligned} U_1(\theta) &= R.i_1(\theta) + \omega.\frac{d\psi_1(i_1,i_2,\theta)}{d\theta} \\ U_2(\theta) &= R.i_2(\theta) + \omega.\frac{d\psi_2(i_2,i_3,\theta)}{d\theta} \\ U_3(\theta) &= R.i_3(\theta) + \omega.\frac{d\psi_3(i_3,i_1,\theta)}{d\theta} \end{aligned} \quad (2)$$

Where $U_1(\theta)$,$U_2(\theta)$ and $U_3(\theta)$ are the applied voltages to phases 1, 2, 3 respectively.
R is the resistance of the winding. i_1, i_2 ,i_3 are the currents of the phases.
Ψ_1, Ψ_2, Ψ_3 are the main fluxes in the stator poles.
ω is the rotor speed considered as constant. θ is the position of the rotor.
The resolution of this non-linear differential system (equation 2) involves determining the flux values at all areas of the motor.

2. Reluctance network method.

The reluctance network method (RNM) presents an ease of use and is very convenient for SRM structure. This method consists in strewing the cross section of the motor with nodes creating meshes over the magnetic circuit. Each node is connected to the next node with a reluctance (figure2). These reluctances represent ferromagnetic areas and non magnetic areas.

Ferromagnetic areas are represented by the reluctances R_{mag} of the teeth and yokes; they are calculated by equation (3):

$$R_{mag} = \frac{l}{h.k_f.\mu.L} \quad (3)$$

l is the length of the area crossed by the magnetic field, h the area width, k_f the stacking factor of steel, L the length of motor, μ the mean value of magnetic area permeability and μ_0 the air permeability.

$$R_{sl} = \frac{l}{h.k_f.\mu_0.L} \quad (4)$$

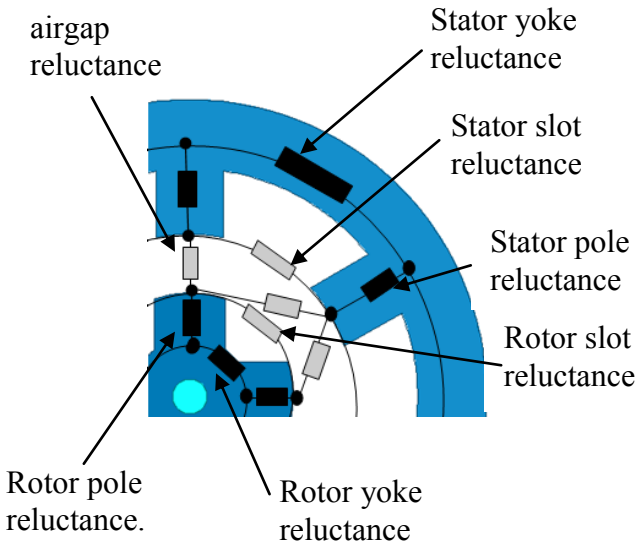

Fig. 2. Reluctances of different parts of SRM.

Non magnetic areas are of two kinds; slots which reluctances R_{sl} are calculated by equation (4), and airgap areas which reluctances will be more difficult to calculate. This difficulty is due to the changing geometry of the airgap according to rotor movement. Choosing teeth contour permeance method makes easier this calculation and takes into consideration airgap geometry and movement.

2.1. Using teeth contour permeance for air gap reluctance calculation.

As said above, calculating airgap reluctances is complex since determining flux paths depends on

airgap configuration and movement. For simplicity, a panoramic airgap configuration is shown in figure 3. Airgap flux paths have tubular form and get into slots at certain depth calculated by CARTER's equation.

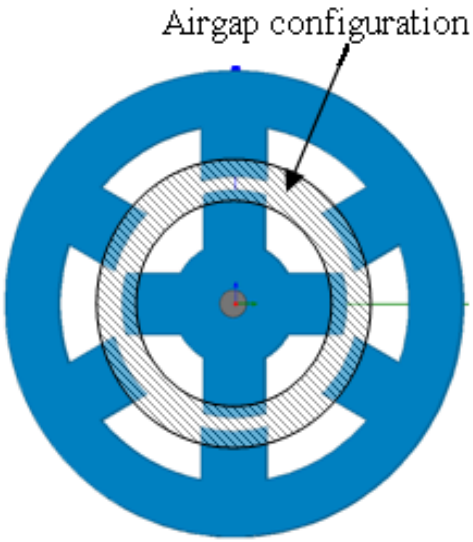

Fig. 3. Radial view of airgap.

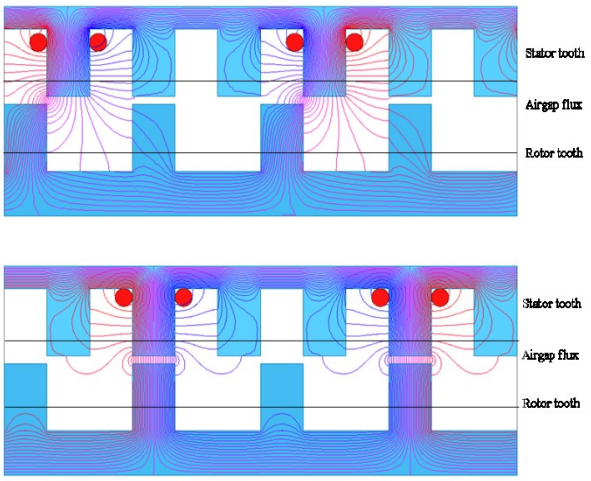

Fig. 4. Panoramic view of airgap for nonaligned and aligned position.

Adapting teeth contours permeance method for such geometrical configuration consists in three essential steps [2]:

1- Determining overlaps bounded by pole axes on both sides of airgap (figure5). For a 6/4 SRM the number of overlaps is 8 or 10 according to rotor position. This leads to 8 or 10 airgap reluctances. Corresponding permeances P_a of each overlap are calculated.

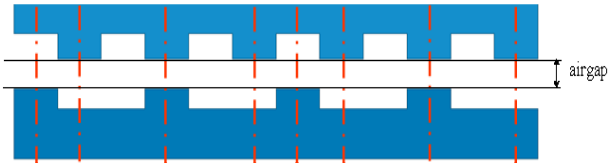

Fig. 5. Panoramic view of airgap and Overlaps regions.

2- While flux tubes get deep into slots as shown in figure4, airgap can be transformed into Carter's smooth air gap(figure6). The permeances P_c are then calculated.

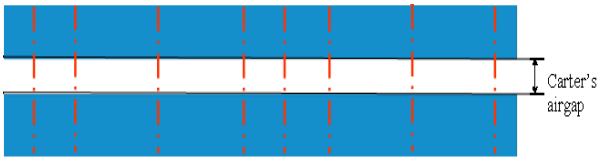

Fig. 6. Panoramic view of CARTER's smooth airgap.

3- Transforming the difference between these two permeances in a triangular-shaped slot (figure7) and calculate its permeance *Pt*. The height (***h***) of the triangle is calculated from equality between the first two permeances.

$$Pt(h) = Pc - Pa \qquad (5)$$

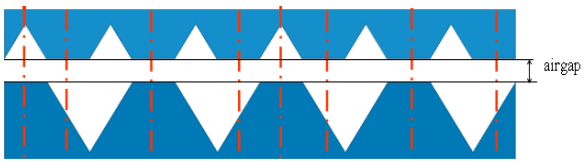

Fig. 7. Panoramic view of triangular airgap.

Determining ***h*** depends on geometry of each overlap. An example of overlap composed of four areas is shown in figure7. The equivalent permeance is the sum of the areas permeances. The rotor displacement leads to a changing airgap where some areas appears and some others disappears…etc. This is why the proposed algorithm takes into account all the possible areas

that can exist for any rotor position.

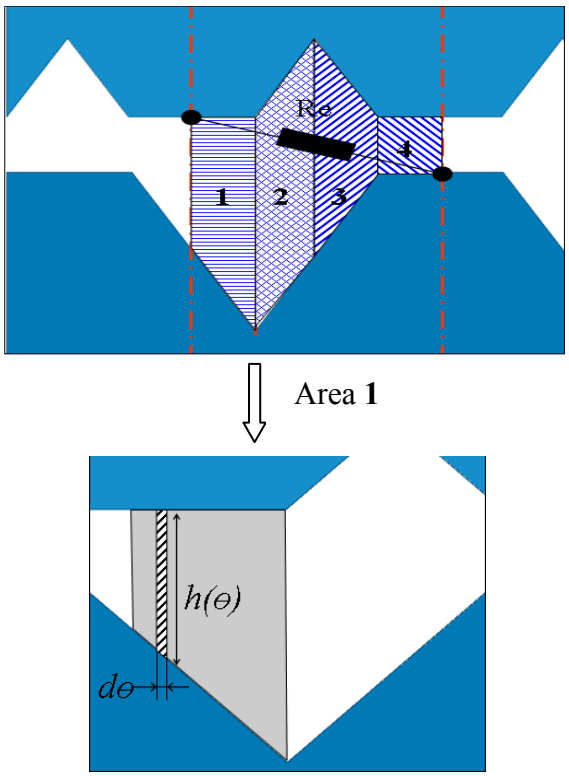

Fig. 8. Configuration of overlaps areas.

On the basis of permeance equation (6), all areas permeances are summed (equation7) and the airgap reluctances are deduced (equation8).

$$dP = \frac{\mu_0 . k_f . L}{h(\theta)} . d\theta \qquad (6)$$

$$Pt(\theta) = Pe_1 + Pe_2 + Pe_3 + Pe_4 \qquad (7)$$

$$Re(\theta) = \frac{1}{Pe(\theta)} \qquad (8)$$

2.2. RNM model and validation.

All reluctances are inserted to the equivalent network illustrated in figure8 which uses analogy to electric networks, by applying the OHM's law for circuits and KIRCHOFF's laws for loops and nodes. The flux, the magneto motive forces and the reluctances are modeled by analogy, respectively to currents, voltages and resistances.

Writing the equations for each mesh using OHM's and Kirchhoff's laws leads to the matrix equation(9).

$$[F] = [R].[\Psi] \qquad (9)$$

[F] is the magneto motive force vector formed by the magnetic forces in each mesh.

[R] is the reluctance matrix formed by the reluctances in each mesh.

[Ψ] is the flux vector formed by the fluxes in each mesh and it is unknown.

For the resolution of this system the iterative Gauss-Sidell method is used.

After determining the inductions in each part of the SRM for a given position, equations (2) is solved for determining induction, current and then calculate torque. For resolution, a NEWTON-RAPHSON method for nonlinear differential equations systems is implemented.

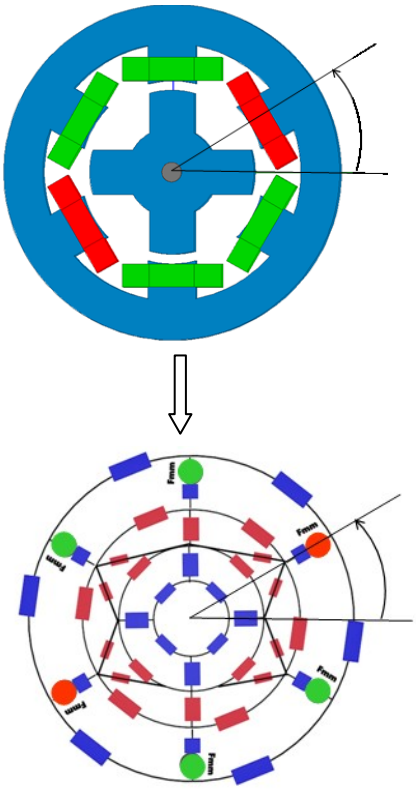

Fig. 9. SRM corresponding reluctance network.

The RNM model set above is compared to finite element model for validation. The tried and tested commercial software Ansoft Maxwell was used. The main fluxes of main stator pole with both methods have been compared. Figure9 shows that RNM model closely matches FEM model. This comparison highlights the reliability of the RNM model. The method also presented a fastness that reduces calculation time. Permeance contour

method described airgap flux with better accuracy than other methods used for airgap reluctance calculation.

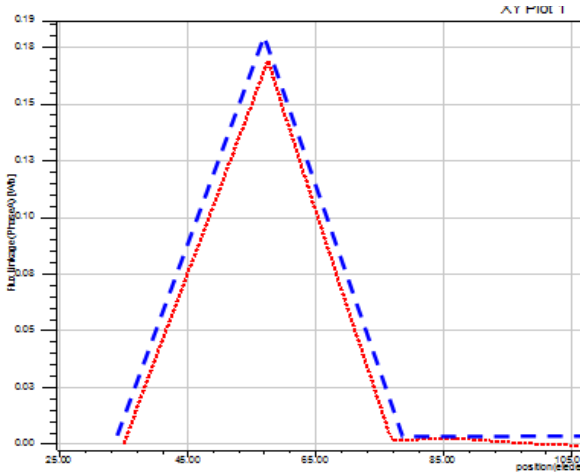

Fig. 10. Induction in main stator pole with RNM method (-----) and FEM (·····).

Dimensions(mm)	stator	rotor
Inner diameter	47	5
Outer diameter	81	46
Teeth height	10	10
Teeth width	10	16
Yoke thickness	10	9
number of poles	6	4
length	150	150
air gap	0.5	
Speed		1000rnd/mn

Table 1. SRM geometrical characteristics.

After validating the model, the design procedure can be started, but first the torque equation must be developed for numerical calculation. It is well known that reluctant torque ***T*** is deduced from the coenergie W' equation which is current and induction dependent [6] and is given by equation (10):

$$W' = \int_0^i \psi di \qquad (10)$$

$$T = \frac{\partial W'}{\partial \theta} \qquad (11)$$

By substitution:

$$T = \frac{\partial}{\partial \theta} \int_0^i \psi di \qquad (12)$$

Finally for numerical calculation of torque equation (13) is used.

$$T = \frac{\sum_{j=0}^{i_2} \psi_j . i_2 - \sum_{j=0}^{i_1} \psi_j . i_1}{\theta_2 - \theta_1} \qquad (13)$$

3. SRM Design procedure and discussion.

The simulations are made on the basis of an existing SRM witch characteristics are given in table 1.

Two groups of simulations are done; constant current and constant voltage supplied SRM. For both, stator teeth, rotor teeth and airgap thickness are varied. All other geometric and electric parameters still unchanged.

Design limits can be listed as below:

- Induction less then 1.8Tesla (value of saturation for the magnetic material).
- current density less than 10A/mm².
- Minimal Torque ripple and maximal mean value.
- In addition construction limits are to be considered; for example an airgap of 0.01mm is not possible neither a rotor teeth of 1 mm because it may weaken mechanically the rotor.

Previous works [1] show that switching angle of -10° gives best shapes and values of torque, so this value is used for all simulations.

3. 1. Constant Current Supplied SRM.

In this part the current is constant and has not to be calculated, the e.m.f is 1000A/t .

Figure (11) shows the torque of the motor for different stator teeth. Enlarging stator teeth leads to a larger torque shape but lower mean value. The same simulations are done for rotor teeth variation figure (12). Diminution of airgap figure (13) gives a better torque shape but lower mean value. Torque is improved by increasing the stator teeth or the rotor teeth and diminution of airgap.

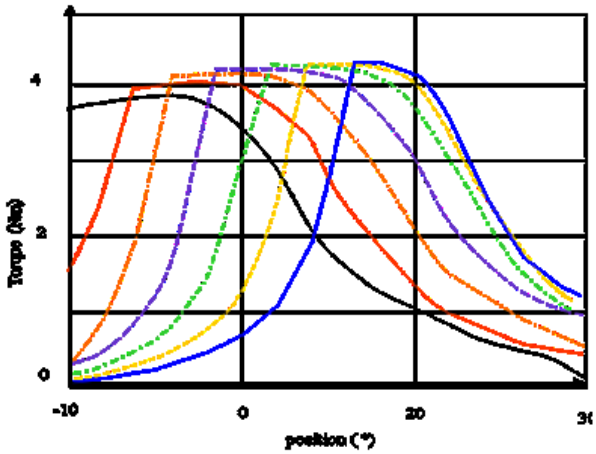

Fig. 11. Torque versus position from stator tooth (βs) 8mm(blue) to 20 mm by step of 2 mm for constant current.

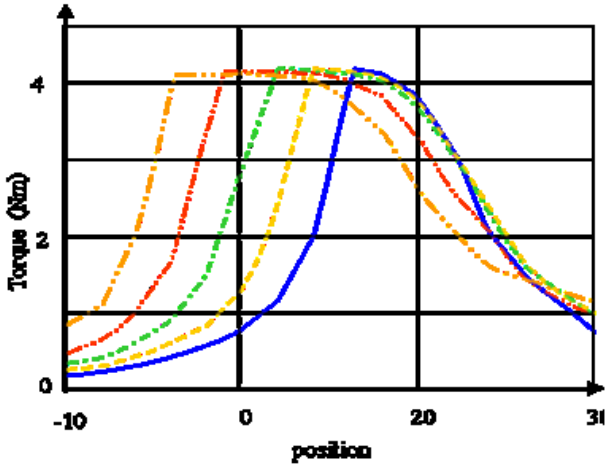

Fig. 12. Torque versus position from rotor tooth (βr) 8mm (in blue) to 16 mm by step of 2 mm For constant current.

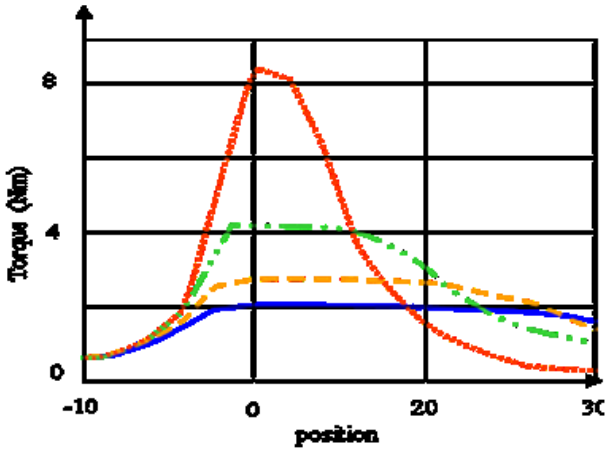

Fig. 13. Torque versus position from airgap 0.25mm (in red) to 1 mm by step of 0.25 mm for constant current.

3.2. Constant Voltage Supplied SRM.

At constant voltage, the current is variable and must be determined, as well as the induction for each position. Simulations also treated effects of changing stator and rotor teeth and airgap. The same results were obtained; enlarging stator or rotor teeth improved the current and torque (figure14). Reducing airgap thickness (figure 15) improved current and torque

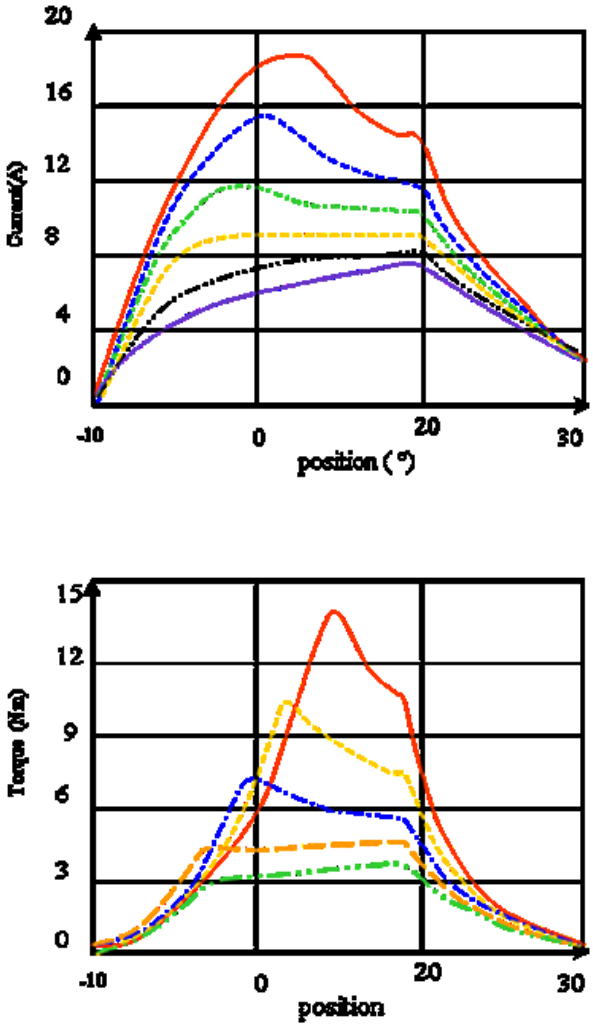

Fig. 14. Currents and Torques versus position from rotor tooth (βr) 8mm (in red) to18 mm by step of 2mm for constant voltage.

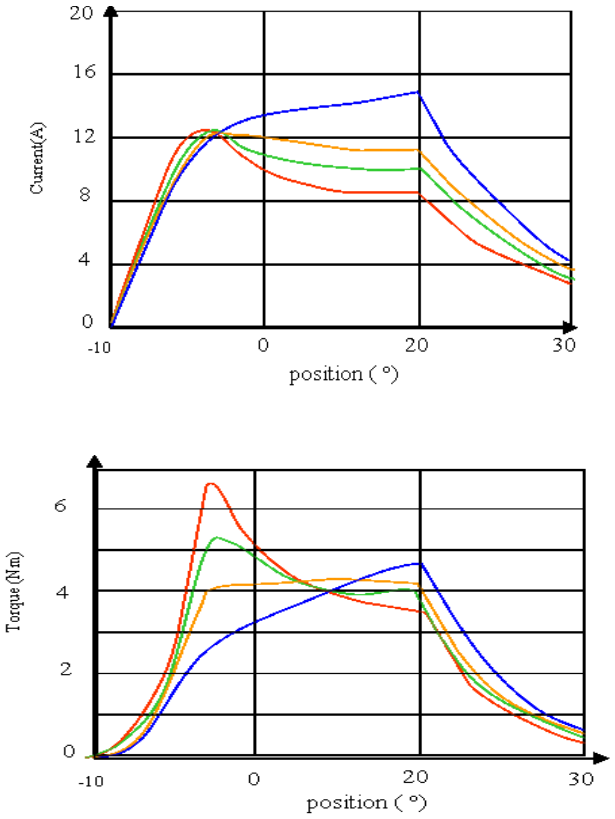

Fig. 15. Currents and torques versus position from airgap of 0.3 mm(in red) to 0.9mm by step of 0.2mm for constant voltage.

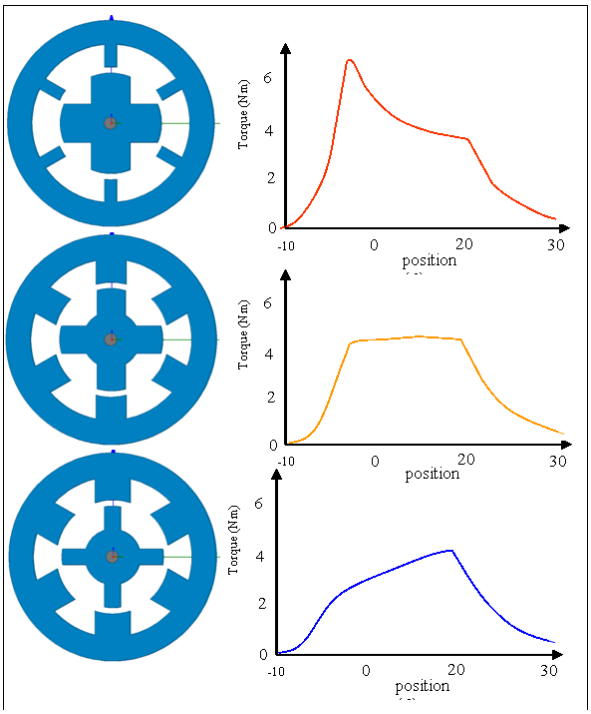

Fig. 16. Geometry and corresponding torque for stator teeth smaller, equal and greater than rotor teeth respectively.

Figure16 shows the cross section for different dimensions of teeth and their relatives' torques; e.g. if stator teeth smaller than rotor teeth torque will be higher but rippled.

The choice of a given geometry is determined by the application considerations and the construction limits.

From the results above, it have been noticed that each stator teeth matches with a rotor teeth to give an optimal value for torque. The same work is repeated for different air gaps and the same relation is deduced each time. At the end of this work an abacus was established for helping design of this volume SRM.. Figure17 shows a relation between rotor and stator teeth for different airgap thickness.

The steps set above can be used as a design methodology to determine dimensions for any SRM and it will be a basis for future works.

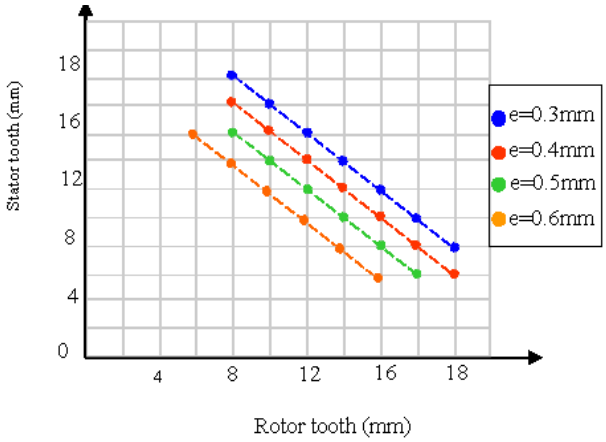

Fig. 17. Rotor teeth versus stator teeth for different airgaps.

4. Conclusion.

A RNM model of switched reluctance motor was set and validated with FEM method. Reluctance network method has presented a reliability and accuracy with considering the nonlinear permittivity of material, the movement and the geometry. This method combined to the teeth contours permeance method has demonstrated its adaptability for salient structures such as SRM. The interest of these two methods is the reduction of calculation time, with high accuracy. We also highlighted the relation that exists between the geometrical parameters and the electromagnetic behavior of the SRM such as torque and current. It means that SRM characteristics can be improved at the stage of construction. Finally, a relation between stator pole and rotor pole dimensions with the air gap as parameter was deduced for the studied SRM.

References

1. Kada Belghitri N., Taieb Brahimi A.and Kernane C.: *Optimization of teeth denture and improvement of torque by supply angle choice*. In: Proceeding of the 3rd national conference on The induction, application of electromagnetic induction, april 24-25-26, 2013,Tizi-Ouzou, Algeria.
2. Kada Belghitri N., Taieb Brahimi A. and Kernane C.: *using reluctance network metod in SRM design. In:* Proceeding of international conference on electrotechnics ICEL2013, 10-11 December 2013 Oran, Algeria.
3. Wei W., Dunlop J B., Collocott S. J., and Kalan B.A.: *Design Optimization of a Switched Reluctance Motor by Electromagnetic and Thermal Finite-Element Analysis*. IEEE vol. 39, no. 5, Sep 2003.
4. Miller T, J, E,: *Optimal design of Switched reluctance motor*. IEEE, vol. 49 no1, Feb 2002.
5. Vijayraghavan P.: *Design of switched Reluctance motors and development of a universal controller for switched reluctance and permanent magnet brushless DC motor drives*. Dissertation, Virginia 2001.
6. Rasmussen P.O.: *Design and Advanced Control of Switched Reluctance Motors*. Dissertation , Aalborg University 2002.
7. Stephenson J. M. and Corda J. :*Computation of torque and current in doubly-salient reluctance motors from nonlinear magnetization data*. In: Proceeding of Institute of Electrical Engineering., vol. 126, no. 5, pp. 393–396, 1979.
8. Miller T. J. E. and Mc Gilp M.: *Nonlinear theory of the switched reluctance motor for rapid computer-aided design*. Proceeding Inst. Elect. Eng.,B, vol. 137, no. 6, pp. 337–347, Nov. 1990.
9. Miller T. J. E, Glinka M., Cossar C., Gallegos-Lopez G., Ionel D., and Olaru M.: *Ultra-fast model of the switched reluctance motor*. In proceeding of Conference Rec. IEEE-IAS Annual Meeting, St. Louis, MO, Oct. 1998, pp. 319–326.